Limnol. Oceanogr., 59(1), 2014, 285–297

doi:10.4319/lo.2014.59.1.0285

Anthropogenic nutrient sources rival natural sources on small scales in the coastal waters of the Southern California Bight

Meredith D. A. Howard,[1,*] Martha Sutula,[1] David A. Caron,[2] Yi Chao,[3,a] John D. Farrara,[3] Hartmut Frenzel,[4,b] Burton Jones,[2,c] George Robertson,[5] Karen McLaughlin,[1] and Ashmita Sengupta [1]

[1] Southern California Coastal Water Research Project, Costa Mesa, California
[2] Department of Biological Sciences, University of Southern California, Los Angeles, California
[3] Joint Institute for Regional Earth System Science and Engineering, University of California, Los Angeles, Los Angeles, California
[4] Department of Atmospheric and Oceanic Sciences, University of California, Los Angeles, Los Angeles, California
[5] Orange County Sanitation District, Fountain Valley, California

Abstract

Anthropogenic nutrients have been shown to provide significant sources of nitrogen (N) that have been linked to increased primary production and harmful algal blooms worldwide. There is a general perception that in upwelling regions, the flux of anthropogenic nutrient inputs is small relative to upwelling flux, and therefore anthropogenic inputs have relatively little effect on the productivity of coastal waters. To test the hypothesis that natural sources (e.g., upwelling) greatly exceed anthropogenic nutrient sources to the Southern California Bight (SCB), this study compared the source contributions of N from four major nutrient sources: (1) upwelling, (2) treated wastewater effluent discharged to ocean outfalls, (3) riverine runoff, and (4) atmospheric deposition. This comparison was made using large regional data sets combined with modeling on both regional and local scales. At the regional bight-wide spatial scale, upwelling was the largest source of N by an order of magnitude to effluent and two orders of magnitude to riverine runoff. However, at smaller spatial scales, more relevant to algal bloom development, natural and anthropogenic contributions were equivalent. In particular, wastewater effluent and upwelling contributed the same quantity of N in several subregions of the SCB. These findings contradict the currently held perception that in upwelling-dominated regions anthropogenic nutrient inputs are negligible, and suggest that anthropogenic nutrients, mainly wastewater effluent, can provide a significant source of nitrogen for nearshore productivity in Southern California coastal waters.

Eutrophication of coastal waters has greatly increased in the last several decades throughout the world, with demonstrated linkages to anthropogenic nutrient loads (*see* reviews Howarth 2008; Paerl and Piehler 2008). Human population growth, development of coastal watersheds, agricultural and aquaculture runoff into the coastal oceans, and burning of fossil fuels are among the many factors contributing to increased eutrophication of coastal waters (Anderson et al. 2002; Howarth 2008). Anthropogenic inputs of agricultural runoff, wastewater and sewage discharge, and groundwater discharge have all been shown to provide significant sources of nitrogen (N) that have been linked to increased primary and macroalgal production (Lapointe et al. 2004, 2005) and harmful algal blooms (HABs) (Anderson et al. 2002; Glibert et al. 2005; Heisler et al. 2008). Anthropogenic nutrient inputs are considered the most significant factor contributing to the global increase in the frequency and intensity of HABs (Hallegraeff 2004; Glibert et al. 2005). Although many studies have focused on agricultural runoff, wastewater has also been found to promote HABs and increase primary productivity (Jaubert et al. 2003); in some regions, wastewater has been shown to be more important than upwelling as a N source (Chisholm et al. 1997; Thompson and Waite 2003; Lapointe et al. 2005).

Nitrogen has been the focus of most coastal eutrophication studies because it has been shown to be the primary limiting macronutrient for algae in coastal waters (Dugdale 1967; Ryther and Dunstan 1971) including California (Eppley et al. 1979). However, previous research has shown that the N form, not just quantity, is important for HABs and algal blooms (Glibert et al. 2006), particularly in California coastal waters (Howard et al. 2007; Cochlan et al. 2008; Kudela et al. 2008).

Recent studies within the Southern California Bight (SCB) have documented chronic algal bloom hot spots that coincide with areas that have potentially significant anthropogenic nutrient inputs (Nezlin et al. 2012). Before 2000, toxic outbreaks of *Pseudo-nitzschia* (an algal diatom that produces domoic acid) were considered rare (Lange et al. 1994); however, in recent years, frequent occurrences (Seubert et al. 2013) and high concentrations of this toxin have been documented in the SCB (Trainer et al. 2000; Schnetzer et al. 2007; Caron et al. 2010) and have been attributed to upwelling (Lewitus et al. 2012; Schnetzer et al. 2013). Increased awareness of toxic HAB events served as the primary motivation for establishment of the Harmful Algae and Red Tide Regional Monitoring Program by the Southern California Coastal Ocean Observing System (SCCOOS). This ongoing program collects weekly HAB species and toxin information from five pier locations in Southern California (SC; data available online, http://www.sccoos.org/data/habs/index.php).

* Corresponding author: mhoward@sccwrp.org

Present addresses:
[a] Remote Sensing Solutions, Pasadena, California
[b] University of Washington, Seattle, Washington
[c] King Abdullah University of Science and Technology, Thuwal Kingdom of Saudi Arabia

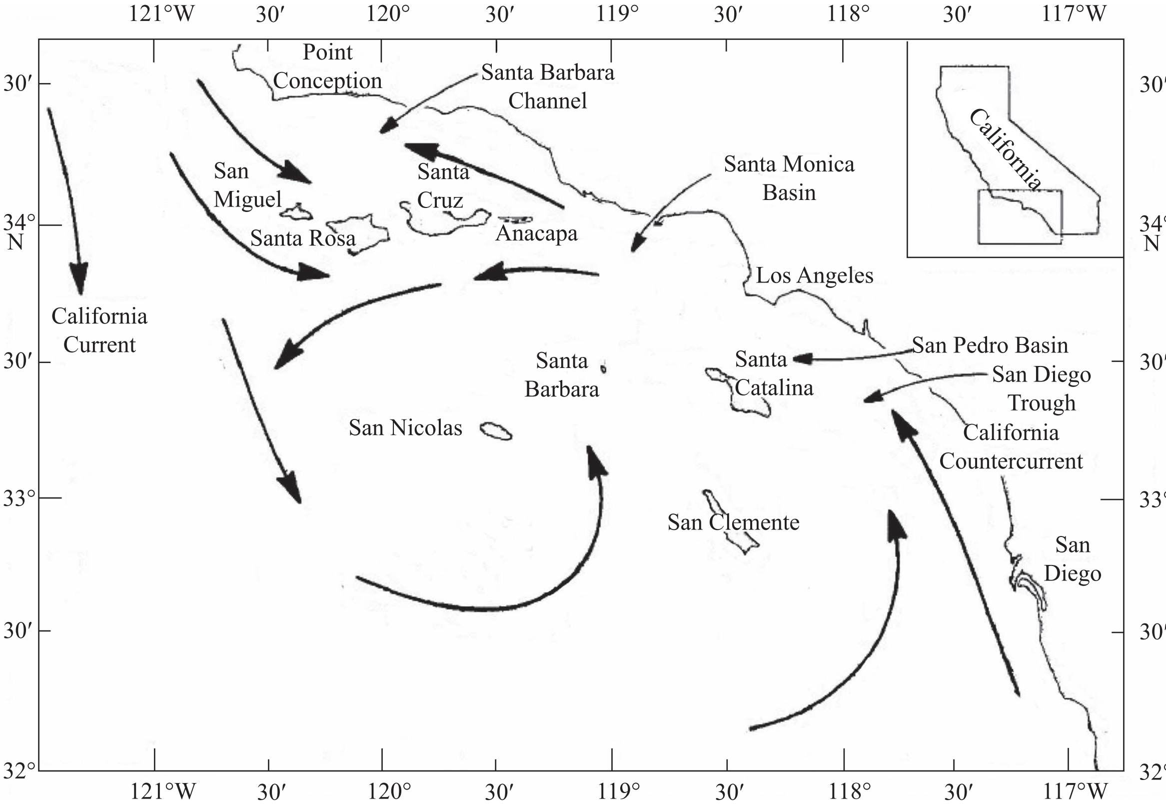

Fig. 1. The circulation patterns in the SCB (adapted from Hickey 1992).

There is a general perception that in upwelling regions, such as coastal California, the flux of anthropogenic nutrient inputs is insignificant relative to upwelling flux, and therefore anthropogenic inputs have relatively little effect on the productivity of coastal waters. Upwelling is the process by which vertical currents transport deep nutrient-rich water to the surface, displacing nutrient-depleted surface water. No studies to date have quantified and compared the natural and anthropogenic inputs on regional and local scales in the SCB to verify the accuracy of this perception. However, a growing number of studies have suggested a linkage between anthropogenic N sources and algal blooms (including HABs) in California (Kudela and Cochlan 2000; Beman et al. 2005; Kudela et al. 2008). Additionally, physiological studies have shown that several common California HAB species are capable of utilizing anthropogenic N forms, such as urea (Cochlan et al. 2008; Kudela et al. 2008), for growth, and toxin production can be increased under these conditions (Howard et al. 2007).

To test the hypothesis that natural sources (e.g., upwelling) greatly exceed anthropogenic nutrient sources to the SCB, this study compared the contributions of N from four major nutrient sources, (1) upwelling, (2) treated wastewater effluent discharged to ocean outfalls, (3) riverine runoff, and (4) atmospheric deposition. This comparison was made using large regional empirical data sets combined with modeling on both regional (SCB-wide) and subregional scales. This is the first study to make this comparison on the U.S. West Coast.

Methods

Study area and circulation patterns—The SCB lies along the southern part of the Pacific coast of the continental United States. The continental coastline generally runs along a north–south gradient beginning at Cape Flattery, Washington (~48°23′N), until Cape Mendocino in northern California (~40°15′N), then turns toward a south–southeast direction. Figure 1 shows the generalized circulation patterns in the SCB. The continuum is broken by a bend or curvature in the coastline between Point Conception (~34°34′N) and the Mexico international border (~32°32′N). The SCB includes an ocean area of 78,000 km^2 (Dailey et al. 1993) and numerous islands offshore. The bottom topography consists of submarine mountains and valleys, neither of which could be considered a classical continental shelf nor a classical continental slope.

A ring of coastal mountain ranges defines SC and shelters the coastal area from dominating northwesterly winds, which create a "coastal basin" where cool, dense air is trapped, resulting in much weaker wind and sea patterns than over the open ocean (Dorman and Winant 1995). SC's climate exhibits relatively dry summer and wet winter seasons. During the dry season a semipermanent eastern Pacific high-pressure area dominates SC. The marine layer is a prominent feature from late spring through early fall. Beginning late fall to early spring (October through March) the high-pressure ridge is displaced and the southern margin of the polar jet stream affects SC. Over 90% of the precipitation generally occurs during this time period.

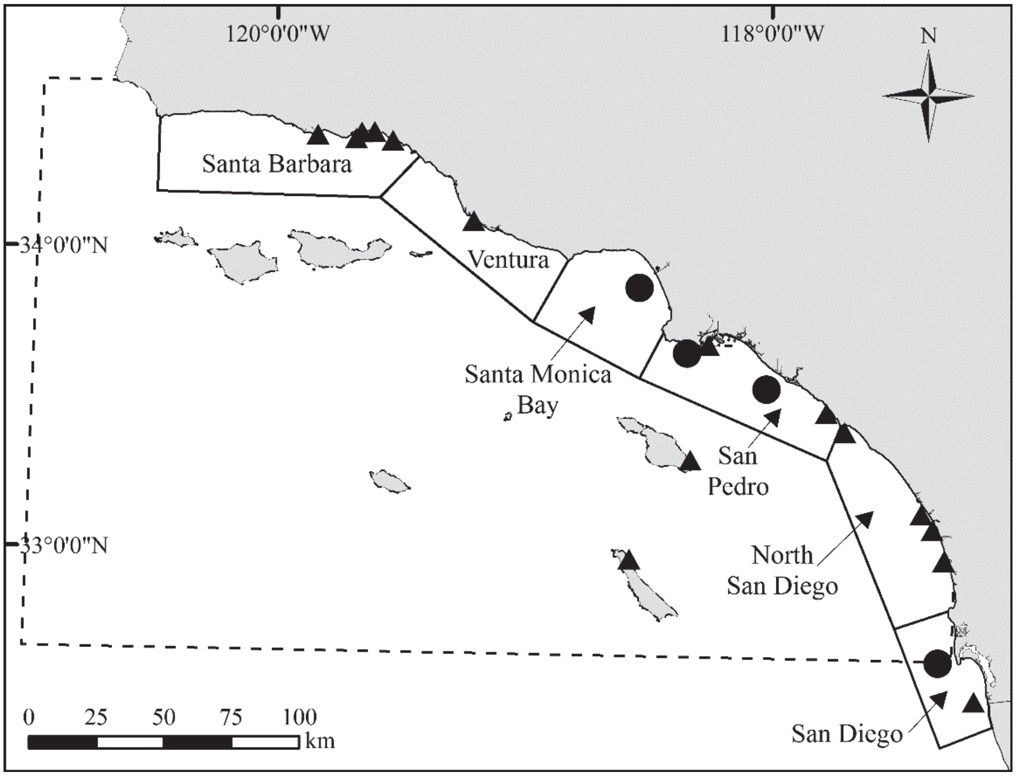

Fig. 2. Regional and subregional SCB boundaries used to calculate fluxes of each of the four major sources. The area used for regional estimates is outlined in a dashed black line; subregions are labeled and outlined in a solid black line. The POTW outfalls that discharge wastewater effluent are represented by black circles for large (> 100 MGD) and black triangles for small (< 25 MGD).

The migratory nature of the region's storm fronts causes alternating periods of dry and wet weather during the rainy season.

The ocean region within the SCB is dominated by the equatorward California Current (CC). The CC is a typical broad eastern boundary current (Hickey 1979) that transports cold subarctic water from north to south throughout the year along a typically narrow (3 to 6 km) coastal continental shelf (Fig. 1). The CC is not steady but migrates seasonally onshore and offshore, producing a rich eddy field (Burkov and Pavlova 1980). As the CC passes Point Conception, it turns south-southeast along SC's outer continental slope, then a portion branches (~32°N) eastward to northward along the coast (Hickey 1992), forming a large gyre known as the Southern California Eddy (Fig. 1). The poleward current along the coast is called the Southern California Countercurrent (SCC) (Sverdrup and Fleming 1941). It transports warm southern water into Santa Monica Bay and the Santa Barbara Channel.

Surface current flows may not reflect subpycnocline currents (Hamilton et al. 2006). During spring, the intensity of the equatorward CC increases compared with the poleward SCC. The CC jet migrates onshore, and the eastward branches penetrate into the SCB through the Santa Barbara Channel and onward south of the Channel Islands (Hickey 1979). The islands act as barriers to deflect surface currents in different directions. Near shore, over the continental shelf and borderland slope, the near-surface flow is commonly equatorward, whereas the California Undercurrent is poleward (Hickey 1992).

Estimation and comparison of nutrient sources—The N fluxes into the SCB from four potential sources were estimated: (1) upwelling, (2) wastewater effluent discharge, (3) riverine runoff, and (4) atmospheric deposition. A combination of field measurements and modeling over a 1-yr period (January–December 2010) was used to estimate the contribution of each nutrient source on a bight-wide scale (51,686 km^2) as well as for six smaller subregional areas (Fig. 2) including: Santa Barbara (2405 km^2), Ventura (1449 km^2), Santa Monica Bay (1571 km^2), San Pedro (1641 km^2), North San Diego (1837 km^2), and San Diego (1020 km^2). The combined area of all of the subregions makes up 20% of the total bight-wide area of the SCB. Nutrient inputs were estimated as annual loads for the bight-wide scale (reported in kg N yr^{-1}) as well as annual fluxes for the six subregional areas (reported as kg N km^{-2} yr^{-1}).

Modeling to estimate upwelling—The upwelling contribution of N was estimated using the regional oceanic modeling system (ROMS), a three-dimensional ocean circulation model for the U.S. West Coast (Marchesiello et al. 2003), coupled with an nutrient–phytoplankton–zooplankton–detritus (NPZD)-type ecosystem–biogeochemistry model (Gruber et al. 2006) to generate a reanalysis of the ocean environment from January to December 2010. This model integration resulted in highly time-resolved output of the three-dimensional physical and biogeochemical parameters. The ROMS model saves output of the daily averages of all advection terms in Eq. 1 (Gruber et al. 2006) and the output was integrated over time and space.

$$\frac{\partial B}{\partial t} = \nabla \cdot K \nabla B - \vec{u} \cdot \nabla_h B - \left(w + w^{\mathrm{sink}}\right) \frac{\partial B}{\partial z} + J(B) \qquad (1)$$

where K is the eddy kinematic diffusivity tensor, and where ∇ and ∇_h are the three-dimensional (3-D) and horizontal gradient operators, respectively. The horizontal and vertical velocities of the fluid are represented by $\vec{u}$ and w, respectively. The w^{sink} represents the vertical sinking rate of the biogeochemical components and $J(B)$ represents the source minus sink term. All of these terms are described in detail in Gruber et al. (2006). From this detailed output, periods of upwelling were determined using vertical velocity, lateral advection, and temperature fields, and then the net mass of nitrate (NO_3) and ammonium (NH_4) from lateral and vertical fluxes to the euphotic zone was calculated. The total vertical flux assimilated by the model includes advection and diffusion, whereas the total lateral flux was assimilated for advection only. Daily estimates were summed to provide an annual estimate. The total flux of N (NO_3 and NH_4) estimates were made over a range of spatial scales, from a bight-wide scale (Fig. 2 black dotted line) to smaller subregional scales (Fig. 2 black solid line).

Model description—ROMS is a free-surface, hydrostatic, 3-D primitive equation regional ocean model (Marchesiello et al. 2003; Shchepetkin and McWilliams 2005). A description and validation of the ROMS model at the 15-km spatial scale has been published (Gruber et al. 2006). This ROMS 3-D model provided both 6 hourly "nowcasts" obtained via assimilation of satellite sea-surface temperature, high-frequency radar surface current velocity, subsurface temperatures, and salinities profiled from Argo floats and gliders as well as daily 72-h forecasts. The ROMS output (for the physics-only model runs) was provided at both the Jet Propulsion Laboratory ROMS web site (http://ourocean.jpl.nasa.gov/SCB) and the SCCOOS web site (www.sccoos.org/data/roms).

The ROMS configuration consisted of a single domain covering the SC coastal ocean from Santa Barbara to San Diego at a resolution of 1 km. The vertical discretization used a stretched terrain-following coordinate (S-coordinate) on a staggered grid over variable topography (Song and Haidvogel 1994). The stretched coordinate allowed increased resolution in areas of interest, such as the thermocline and bottom boundary layers. ROMS used a sigma-type vertical coordinate in which coordinate surfaces followed the bottom topography. In the SCB configuration, there were 40 unevenly spaced sigma surfaces used, with the majority of these clustered near the surface to better resolve processes in the mixed layer. The horizontal discretization used a boundary-fitted, orthogonal curvilinear formulation. Coastal boundaries were specified as a finite-discretized grid via land and sea masking. The SCB configuration of ROMS has been tested and used extensively (Dong et al. 2009).

Boundary conditions for the SCB domain were provided from a separate data-assimilating ROMS domain that covered the entire coast of California and northern Baja California at a resolution of 3 km. The tidal forcing was added through lateral boundary conditions that were obtained from a topography experiment–Poseidon (TOPEX POSEIDON) global barotropic tidal model (TOPEX POSEIDON global barotropic tidal model.6; Egbert et al. 1994), which had a horizontal resolution of 0.25° and used an inverse modeling technique to assimilate satellite altimetry crossover observations. There were eight major tide constituents used at the diurnal and semidiurnal frequencies (M2, K1, O1, S2, N2, P1, K2, and Q1). The atmospheric forcing required by the ROMS model was derived from hourly output from forecasts performed with a regional atmospheric model, the Weather Research and Forecasting System (WRF). This model has been used in the SCB region (Conil and Hall 2006). The horizontal resolution was 4 km and the lateral boundary forcing and initial conditions were derived from the National Centers for Environmental Prediction 12-km North American model daily Greenwich mean time forecasts. The surface latent and sensible heat fluxes, as well as surface evaporation rates, were derived from WRF surface air temperatures, surface relative humidity, 10-m winds, solar and terrestrial radiation, and ROMS sea-surface temperatures, using the bulk formula proposed by Kondo (1975). The freshwater flux was computed as the calculated evaporation rate minus the WRF precipitation rate (evaporation − precipitation). The wind stress was derived from the 10-m winds using the formula of Large and Pond (1981). The variables used for computing the ocean-model forcing have been evaluated against buoy data. The surface winds were accurate, with root mean square errors of 2–3 m s^{-1} in speed and 30° in direction. Comparison of modeled vs. measured surface air temperatures and relative humidity showed good accuracy with errors of 1–2°C and 5–10%.

The biogeochemical model that was used in this ROMS configuration was an NPZD model based on Fasham et al. (1990). The model was optimized and validated for the U.S. West Coast coastal upwelling region by Gruber et al. (2006). This model has been validated and gave good results in the upwelling-dominated coastal zone, but it failed to reproduce observations farther offshore in more nutrient-depleted areas (Gruber et al. 2006). A full description of the model can be found in Gruber et al. (2006), but is described briefly here.

The NPZD model included a single limiting nutrient (N) and a diatom-like single phytoplankton class. Although the model output was only used to calculate NO_3 and NH_4 lateral and vertical fluxes, a total of 12 state variables is tracked including: NO_3, NH_4, phytoplankton, zooplankton, small and large detritus (both N and carbon [C] concentrations due to varying C : N ratios), oxygen, dissolved inorganic carbon, calcium carbonate, and total alkalinity.

In the absence of a larger domain model with the same NPZD biogeochemical model characteristics, biogeochemical boundary conditions were based on the physical

Table 1. List of polynomial (polyn.) parameters for the biogeochemical boundary conditions in ascending order, e.g., $NO_3(\sigma_\theta > 26.8) = -20{,}258 + 1484.7\sigma_\theta - 27.1422\sigma^2$. Chlorophyll *a* (Chl *a*), not applicable (na).

Variable	σ_θ range 1	Polyn. 1	σ_θ range 2	Polyn. 2	σ_θ range 3	Polyn. 3
Nitrate	Up to 24.99	−48.0343, 1.9910	25.0–26.79	−371.8125, 11.3264, 0.1449	Over 26.8	−20258, 1484.7, −27.1422
Chl *a* (top 50 m)	All values	−547.1559, 42.7240, −0.8334	na	na	na	na
Chl *a* (>50 m)	All values	17.4953, −0.7332	na	na	na	na
Ammonium	Up to 24.82	−1.9986, 0.0866	24.82–26.42	−265.6287, 20.7761, −0.4056	26.42–27.2	170.3260, −12.5235, 0.2302

boundary conditions, modeled at daily time steps, and the relationship between physical quantities (either temperature or potential density) and nutrients were used to derive initial and boundary conditions for NO_3 and NH_4, as summarized in Table 1. There were not enough organic N or urea data to estimate the contribution of this form from upwelling. Therefore the total dissolved nitrogen (TN) flux for upwelling excludes organic N sources. Initial and boundary conditions for NO_3 concentrations were determined with a polynomial regression that describes the relationship between NO_3 and density (σ_θ), defined for the SCB from temperature, salinity, and NO_3 data from the World Ocean Atlas 2005 (Garcia et al. 2006; Fig. 3).

Climatological biogeochemical boundary and initial conditions were used to determine a relationship between potential density and NH_4 because there were no observed data available for NH_4. The scatter is much larger for this relationship than for NO_3 (Fig. 3).

Wastewater effluent discharge—Nutrient loads from wastewater effluent discharged from outfalls to the SCB were estimated for both large (> 100 million gallons a day [MGD]) and small (< 25 MGD) publicly owned treatment works (POTWs) in each subregion (Table 2), where large POTWs contribute 90% of total discharges to SCB. Large POTW nutrient loads were determined for January–December 2010 by measuring effluent nutrient concentrations quarterly from December 2008 through December 2009; these quarterly concentrations were combined with monthly discharge flows from 2010 National Pollutant Discharge Elimination System (NPDES) monitoring reports from the Hyperion Treatment Plant (HTP) operated by City of Los Angeles (LA), the Joint Water Pollution Control Plant (JWPCP) operated by LA County Sanitation District, the Treatment Plant No. 2 operated by Orange County Sanitation District, and the Point Loma Wastewater Treatment Plant operated by City of San Diego. Samples were analyzed for TN following Environmental Protection Agency (EPA) method SM4500-N, nitrate plus nitrite (herein referred to as NO_3) following EPA 300.0 and SM4500, ammonia (NH_3) following method EPA 350.1 and SM4500, and urea using Goeyens et al. (1998). Organic nitrogen (ON) was not measured for the large POTWs, only urea, which is a component of ON. An interlaboratory comparison was conducted for these analytes and the variability was determined to be negligible.

Effluent nutrient concentration data for small POTWs were determined using available data published for 2005 from NPDES monitoring reports (Lyon and Stein 2008). Small POTW effluent concentration data were available for NO_3, NH_3, and TN; ON was reported from one POTW in Ventura. Details on methods were reported in Lyon and Stein (2008).

POTW N load (bight-wide) was estimated by multiplying nutrient concentrations (mg L^{-1}) with annual flow volume (L) and POTW N fluxes for each subregion were estimated by dividing the N load by the area (km^{-2}).

The error associated with the N loads was determined by multiplying the standard deviation (SD) of nutrient concentrations by the total annual discharge. Total error was calculated as the square root of the squared sums of each of the individual estimates for each watershed.

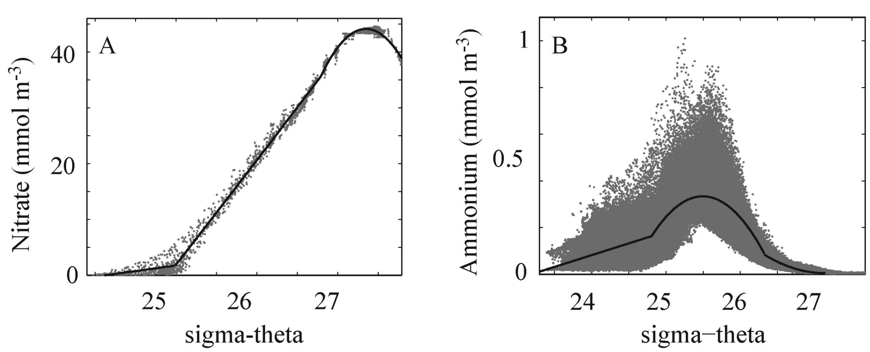

Fig. 3. Relationship between potential density (σ_θ) and (A) nitrate and (B) ammonium in the SCB. Nitrate and ammonium data (gray dots) are derived from the World Ocean Atlas (2005) and ROMS tests run with climatological boundary conditions, respectively. Black lines designate the stepwise polynomial fits.

Table 2. Location and relative size of POTWs used for effluent discharge load estimates by subregion. S, small; L, large; WWTP, wastewater treatment plant.

Subregion	POTW name	Size
Santa Barbara	Goleta WWTP	S
	El Estero WWTP	S
	Montecito WWTP	S
	Summerland WWTP	S
	Carpinteria WWTP	S
Ventura	Oxnard WWTP	S
Santa Monica Bay	HTP	L
San Pedro	JWPCP	L
	Treatment Plant No. 2	L
	Terminal Island WWTP	S
	Aliso Creek Ocean Outfall	S
North San Diego	San Juan Creek Ocean Outfall	S
	Oceanside WWTP	S
	Camp Pendleton WWTP	S
	Fallbrook Public Utility District WWTP	S
	Encina Ocean Outfall	S
	San Elijo Water Pollution Control Facility	S
San Diego	Point Loma Wastewater Treatment Plant	L
	Hale Ave. Resource Recovery Facility	S
	South Bay Water Reclamation Plant	S
	International Wastewater Treatment Plant	S

$$\text{Total load SD} = \left(\sum_{1}^{10} [C_e Q]^2\right)^{1/2} \quad (2)$$

where C_e is the standard deviation in nutrient concentration for each large POTW effluent. Q is the total annual discharge.

Riverine loads—Riverine nutrient loads to the SCB were estimated using empirical wet-weather and dry-weather data for monitored watersheds in combination with modeled wet-weather loads for unmonitored watersheds for the period of October 2008–October 2010.

Discharge and nutrient samples were collected at 34 wet-weather and 57 dry-weather mass emission stations by Ventura, Los Angeles, Orange, and San Diego counties under their NPDES permits or by SCB Regional Monitoring Program partners during the period of October 2008–October 2010. Howard et al. (2012) provides methodological details including summary of the wet- and dry-weather monitoring and the 91 mass loading stations utilized for the study.

A spreadsheet model based on the rational method (O'Loughlin et al. 1996) was used to generate freshwater runoff Q ($m^3\ d^{-1}$) and the N loads associated with wet-weather events. Modeled storm discharge (Q) was calculated as a function of drainage area (A, km^2), mean rainfall intensity (I, mm d^{-1}), hydraulic runoff coefficient (C), and conversion constant (k):

$$Q = AICk \quad (3)$$

Hydraulic runoff coefficient (C) varied as a function of land use and cover type (Howard et al. 2012). The Ackerman and Schiff model (2003) was improved by refining land use-specific runoff concentrations for NO_3 (excluding nitrite) and NH_4, on the basis of published values from previously published studies (Stein et al. 2007) and TN runoff concentrations were derived from empirical data for this study (Howard et al. 2012).

Within each watershed, Q was then calculated as the sum of discharge associated with six land-use categories: agriculture, commercial, industrial, open space (natural), residential, and other urban. The daily nutrient loads were estimated as the sum of the product of the runoff concentration (c) and Q for each land use, using Eq. 3.

The error associated with the N loads was determined by multiplying the standard deviation of nutrient concentrations by the total discharge (wet- or dry-weather discharge, respectively, for the watershed). Total error was calculated as the square root of the squared sums of each of the individual estimates for each watershed, as given in Eq. 3.

The drainage area was delineated for each watershed on the basis of hydraulic unit code boundaries. The model domain included all SC coastal watersheds in San Diego, Orange, Riverside, Los Angeles, San Bernardino, Ventura, and Santa Barbara counties with an initial total watershed area of 27,380 km^2. Watershed areas larger than 52 km^2 upstream of dams were excluded in the model domain, to mimic the retention of water by dams (Ackerman and Schiff 2003). The final model domain was comprised of 98 watersheds with a total area of 14,652 km^2. Each of the watersheds was populated with land-cover data from Stein et al. (2007), and aggregated into the six land-use categories.

Daily precipitation data for approximately 200 rain gauge stations were obtained from the National Oceanic and Atmospheric Administration (NOAA), National Environmental Satellite, Data and Information Service, National Climatic Data Center, and Climate Data Online database. Data were transformed to estimate mean precipitation over the 98 watersheds relevant to the study. Precipitation data were interpolated within each watershed on a regular grid using a biharmonic spline interpolation method (Sandwell 1987).

A model scenario was run to estimate the anthropogenic influence on nutrient fluxes to the SCB using 100% open-space land use for the entire Bight, representing a "preurbanization" baseline. The model domain was expanded to include areas above existing dams because there were no dams withholding potential runoff in the modeled preurbanized state. Rainfall data were not available for the period representing the preurbanized state; therefore, current rainfall data (2008–2009) were used to estimate loads. This enabled a comparison of pre- and posturbanization loads without any bias due to differences in precipitation (Howard et al. 2012).

Atmospheric deposition—Atmospheric deposition rates were estimated for both wet-weather and dry-weather deposition. The wet deposition rates were calculated from the average annual rates for 2009 and 2010 at two National

Atmospheric Deposition Program sites: Site 42, Los Angeles County (Tanbark Flat, 34.2071, −117.7618) and Site 94, San Bernardino County (Converse Flats, 34.1938, −116.9131). Wet deposition rates for NO_3 and NH_4 from these two sites were averaged across sites and years (kg km^{-2} d^{-1}), then applied to the total number of wet days for the January–December 2010 study year.

Sampling for dry deposition was conducted three times over a 6-month period at rooftop location at the HTP and the City of Oceanside Library. Techniques using surrogate surfaces for estimating N dry deposition in semiarid environments, including a water surface sampler and filter samplers, were used (Moumen et al. 2004; Raymond et al. 2004). Both of these techniques use aerodynamic discs, are of short duration (2 to 4 d), and produce reproducible results when evaluated against the atmospheric concentrations and each other. Samplers were deployed in duplicate for the water collector and in triplicate for the filter collectors. Filter samplers and water surface samplers were analyzed for NH_4 and NO_3. Concentrations were converted to deposition rates by incorporating the surface area of the sampler and the duration of the sampling event (kg km^{-2} d^{-1}). The average deposition rate for the three sampling events was multiplied by the number of dry-weather days during the January–December 2010 study year for a bight-wide estimation of dry deposition. Results from the HTP site were applied to the Santa Monica Bay and San Pedro Bay subregions, and results from the Oceanside sampler were applied to all other subregions.

Estimates of contribution of anthropogenic activities to SCB nutrient loads—The contribution of anthropogenic activities to SCB nutrient loads was calculated from the total flux of N from natural sources (upwelling, atmospheric deposition, and preurbanization rivers) compared with the TN flux of all nutrient sources (upwelling, atmospheric deposition, posturbanization rivers, and wastewater effluent discharge).

Results

Bight-wide regional nitrogen loads—Summed across the entire SCB scale, TN loads differed by an order of magnitude, with upwelling contributing the largest load and riverine runoff the smallest (Fig. 4, Table 3). Upwelling consisted almost entirely of NO_3 (98.7%), and little NH_4 (1.3%), whereas effluent loads consisted mostly of NH_4 (92%) with minor percentages of NO_3 (7.0%) and ON (1.0%). The riverine runoff was comprised mostly of ON (60%) and NO_3 (35%), with a smaller contribution from NH_4 (6.0%). The NO_3 loads from riverine runoff and effluent were equivalent (3.5×10^6 and 3.4×10^6 kg N yr^{-1}, respectively), even though NO_3 comprised only 7.0% of the TN from effluent. The error analysis of TN loads for the riverine runoff and effluent ranged from 3.3% to 17.6% for effluent and 2.4% to 37.8% for riverine runoff (Table 4).

Subregional nitrogen fluxes—TN for each source varied by subregion. Effluent and upwelling had similar annual TN fluxes for the three subregions with large POTW outfall discharges (Santa Monica Bay, San Pedro, and San Diego; Fig. 5, Table 5). These were 9.9×10^3 and 1.0×10^4 kg N km^{-2} yr^{-1}, respectively, for Santa Monica Bay, 1.2×10^4 and 2.3×10^4 kg N km^{-2} yr^{-1}, respectively, for San Pedro Bay, and 7.4×10^3 and 2.4×10^3 kg N km^{-2} yr^{-1} for San Diego subregion. Note that the upwelling flux estimated for San Diego is at the edge of the model boundary; therefore, it has a large amount of uncertainty. For these three regions, riverine runoff and atmospheric deposition were one to two orders of magnitude less than upwelling and effluent, respectively, with annual fluxes ranging from 7.0×10^1 to 6.0×10^3 kg N km^{-2} yr^{-1} for riverine runoff and 4.3×10^2 to 8.7×10^2 kg N km^{-2} yr^{-1} for atmospheric deposition.

The Santa Barbara and Ventura subregions both had net annual downwelling rather than net upwelling, ranging from 2.1×10^4 to 1.0×10^5 kg N km^{-2} yr^{-1}, respectively. In these subregions, the dominant sources varied from effluent and atmospheric deposition in Santa Barbara (1.6×10^2 and 4.3×10^2 kg N km^{-2} yr^{-1}, respectively) to roughly equivalent fluxes of effluent, riverine runoff, and atmospheric deposition in Ventura (5.1×10^2, 4.1×10^2 and 8.7×10^2 kg N km^{-2} yr^{-1}, respectively). Only in North San Diego County was upwelling (3.6×10^4 kg N km^{-2} yr^{-1}) dominant by an order of magnitude over effluent (1.4×10^3 kg N km^{-2} yr^{-1}) and by two orders of magnitude over riverine runoff (6.0×10^2 kg N km^{-2} yr^{-1}) and atmospheric deposition (4.7×10^2 kg N km^{-2} yr^{-1}).

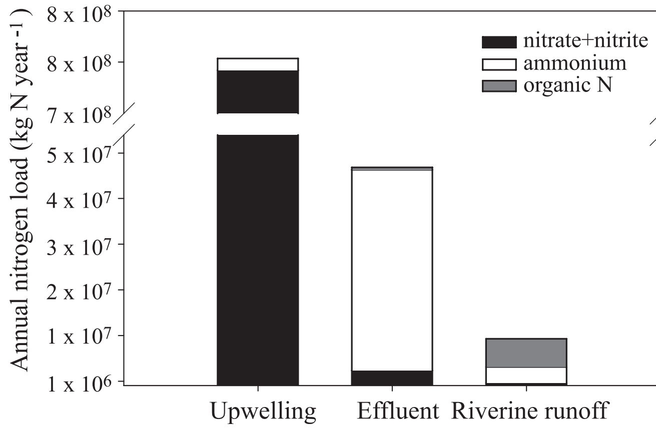

Fig. 4. Annual total nitrogen loads (in kg N yr^{-1}) to the SCB for each nutrient source, with total nitrogen components separated into nitrate plus nitrite shown by the black bars, ammonium shown by the white bars, and organic nitrogen shown by the gray bars.

Table 3. Annual nitrogen loads for each nutrient source and constituent. All loads are 10^6 kg N yr^{-1}. The form of nitrogen expressed as a percentage of total nitrogen for each source is given in parentheses.

	Total N	Nitrate + nitrite	Ammonium	Organic N
Upwelling	750	740 (98.7)	10 (1.3)	na*
Effluent	48	3.4 (7.0)	44 (92.0)	0.5 (1.0)
Riverine runoff†	10	3.5 (34.0)	0.6 (6.0)	6.2 (60.0)

* na, not analyzed for this source.
† Data for January through October 2010.

Table 4. Summary of the standard error calculated for nitrogen components of riverine runoff and effluent. Absolute and standard error are reported as 10^4 kg N yr^{-1}.

	Riverine runoff					
	Wet weather		Dry weather		Effluent	
Component	Absolute error	% error	Absolute error	% error	Standard error	% error
Total N	22	8.8	3.0	2.4	200	4.6
Nitrate	8.4	7.5	2.7	3.6	55	17.6
Ammonium	9.4	37.8	0.8	11.6	130	3.3

The flux of individual forms of nitrogen (NO_3 and NH_4) were estimated for each source in every subregion, whereas ON was estimated when data were available (Table 6). In the Santa Barbara subregion, the largest source of NO_3 is from atmospheric deposition (2.1×10^2 kg N km^{-2} yr^{-1}), whereas effluent and atmospheric deposition deliver equivalent amounts of NH_4 (1.6×10^2 and 2.1×10^2 kg N km^{-2} yr^{-1}, respectively). Riverine runoff and atmospheric deposition deliver the largest fluxes of NO_3 (3.5×10^2 and 2.1×10^2 kg N km^{-2} yr^{-1}, respectively) in Ventura, whereas NH_4 fluxes were dominated by effluent and atmospheric deposition (4.0×10^2 and 2.1×10^2 kg N km^{-2} yr^{-1}, respectively). The highly urbanized areas of Santa Monica Bay and San Pedro exhibited similar flux patterns, with upwelling providing the highest flux of NO_3 (9.3×10^3 and 2.2×10^4 kg N km^{-2} yr^{-1}, respectively), effluent providing the highest flux of NH_4 (8.4×10^3 and 1.2×10^4 kg N km^{-2} yr^{-1}, respectively), and riverine runoff providing the highest flux of ON (1.3×10^2 and 5.0×10^2 kg N km^{-2} yr^{-1}, respectively). The North San Diego subregion had an NO_3 flux from upwelling that was two to four orders of magnitude higher than any other source, whereas upwelling and effluent contributed most of the NH_4 flux (3.1×10^3 and 1.4×10^3 kg N km^{-2} yr^{-1}, respectively). In the San Diego subregion, upwelling and riverine runoff provided the highest flux of NO_3 (1.7×10^3 and 1.5×10^3 kg N km^{-2} yr^{-1}, respectively), whereas effluent provided most of the NH_4 flux (7.3×10^3 kg N km^{-2} yr^{-1}) and ON was mostly provided by riverine runoff (4.2×10^3 kg N km^{-2} yr^{-1}).

Estimates of contribution of anthropogenic activities to SCB nutrient loads—The contribution of anthropogenic activities to SCB nutrient loads was estimated from the TN flux from natural sources (upwelling, atmospheric deposition, and preurbanization rivers) compared with the TN flux of all nutrient sources (upwelling, atmospheric deposition, posturbanization rivers, and wastewater effluent discharge). The increase in TN due to anthropogenic sources was largest for the more heavily urbanized areas of Santa Monica Bay

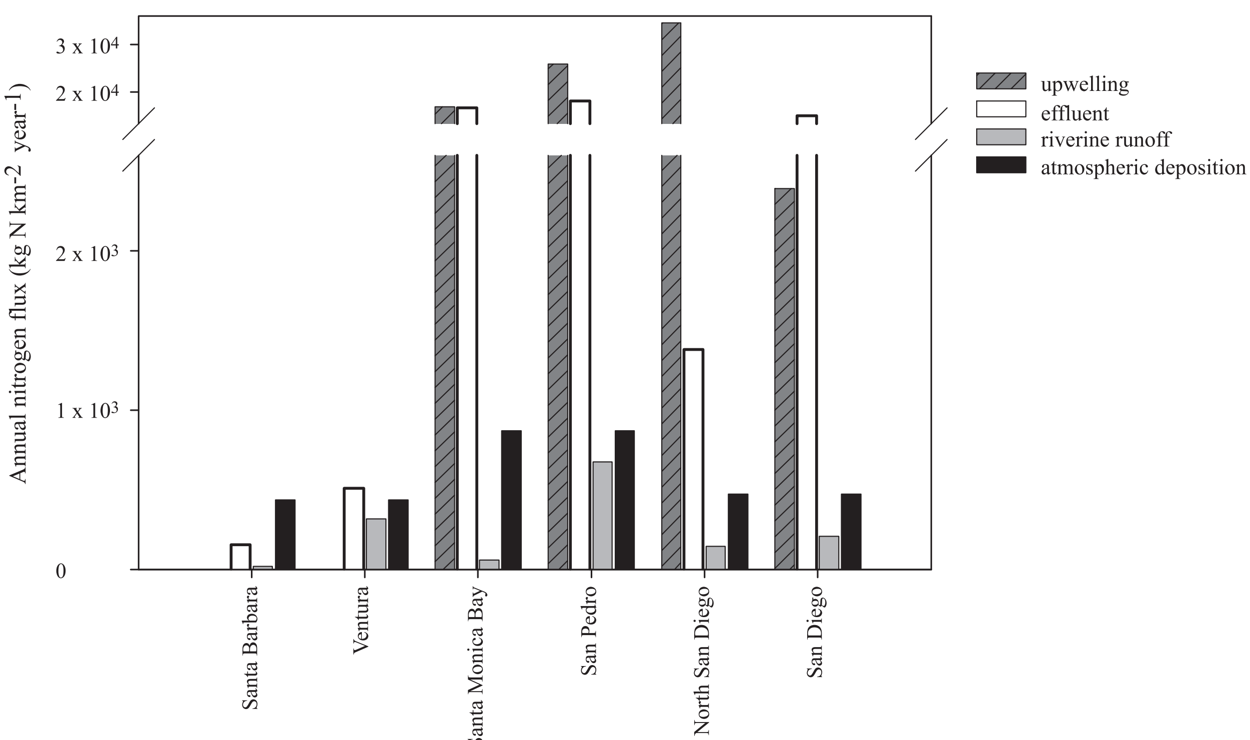

Fig. 5. Total annual nitrogen flux for each subregion in the SCB for each source including upwelling shown by dark gray bars with lines, effluent shown by white bars, riverine runoff shown by light gray bars, and atmospheric deposition shown by black bars.

Table 5. Annual total nitrogen flux for each subregion (10^2 kg N km^{-2} yr^{-1}).

Source	Santa Barbara	Ventura	Santa Monica Bay	San Pedro	North San Diego	San Diego
Upwelling	−210	−1071	102	238	367	24
Effluent	1.6	5.1	99	121	14	74
Riverine runoff*	0.7	4.1	1.4	12	6	60
Atmospheric deposition	4.3	4.3	8.7	8.7	4.7	4.7
Total N	−203	−1057	211	380	392	163

* Data for January through October 2010.

and San Pedro subregions, with increases of 2- and 1.5-fold (110% and 52%), respectively. The less urbanized subregions of Santa Barbara, Ventura, and North San Diego only had slight changes of 5% or less (Table 7).

Discussion

Regional nitrogen loads and subregional nitrogen fluxes—At the scale of the entire SCB region, the results of this study support the hypothesis that natural N sources (i.e., upwelling) dominated anthropogenic sources of N by an order of magnitude (Table 3, Fig. 4). However, at a subregional scale and proximal to the coastline (~20 km), anthropogenic N sources, particularly wastewater effluent discharged through ocean outfalls, were equivalent to natural N sources in five of the six subregions (Table 5, Fig. 5). In the highly urbanized subregions of Santa Monica Bay and San Pedro, anthropogenic N inputs (mainly wastewater effluent) doubled the amount of TN flux in these subregions. The upwelling and effluent sources combined comprised 95% of the TN load in these subregions. The Santa Monica Bay subregion had equivalent contributions from upwelling and wastewater effluent to the TN flux (each was 47% to the TN flux). In San Pedro, the TN contribution from upwelling was the same order of magnitude as wastewater effluent, but the actual upwelling flux comprised 60% of the TN, whereas the

Table 6. Flux of each nitrogen form in each subregion of the SCB (10^2 kg N km^{-2} yr^{-1}).

	Total N	Nitrate + nitrite	Ammonium	Organic N (urea only)
Santa Barbara				
Upwelling	−210	−198	−11	na
Effluent	1.6	na	1.6	na
Riverine runoff	0.7	0.1	0.04	0.6
Atmospheric deposition	4.3	2.1	2.1	na
Ventura				
Upwelling	−1071	−995	−75	na
Effluent	5.1	0.4	4.0	0.7
Riverine runoff	4.1	3.5	0.1	0.4
Atmospheric deposition	4.3	2.1	2.1	na
Santa Monica Bay				
Upwelling	102	93	8.6	na
Effluent	99	13	84	(0.9)
Riverine runoff	1.4	0.001	0.1	1.3
Atmospheric deposition	8.7	6.1	2.4	na
San Pedro				
Upwelling	238	220	18	na
Effluent	121	5.8	121	1.0
Riverine runoff	12	6.3	1.0	5.0
Atmospheric deposition	8.7	6.1	2.4	na
North San Diego				
Upwelling	367	336	31	na
Effluent	14	0.06	14	na
Riverine runoff	6.0	2.2	0.35	3.4
Atmospheric deposition	4.7	2.1	2.1	na
San Diego				
Upwelling	24	17	6.5	na
Effluent	74	2.1	71	(0.6)
Riverine runoff	60	15	3.1	42
Atmospheric deposition	4.7	2.1	2.1	na

na, not analyzed for this source.

Table 7. The total nitrogen flux (10^2 kg N km^{-2} yr^{-1}) for natural nutrient sources (upwelling, atmospheric deposition, and preurbanization riverine runoff) and for natural and anthropogenic sources (upwelling, atmospheric deposition, posturbanization riverine runoff, and wastewater effluent discharge) to the SCB.

	Natural sources	Natural and anthropogenic sources	% change
Santa Barbara	−200	−203	1
Ventura	−990	−1057	7
Santa Monica Bay	100	211	110
San Pedro	250	380	52
North San Diego	370	392	6
San Diego	30	163	nd

nd, not determined due to subregional area at the edge of the ROMS model boundary.

POTW effluent was 33% of TN contribution (Table 5, Fig. 5). The TN flux from riverine runoff and atmospheric deposition was one to two orders of magnitude less than upwelling and effluent in both of these subregions (Table 5, Fig. 5). There are POTWs in these subregions that discharge directly into the major rivers and those discharges were included in the riverine runoff component, thereby making the total contribution of effluent slightly underestimated. In contrast, the North San Diego subregion had least amount of anthropogenic N inputs and the upwelling flux had the highest contribution to TN by two to four orders of magnitude compared with effluent, riverine runoff, and atmospheric deposition (Table 5, Fig. 5). The TN flux in Santa Barbara and Ventura was mostly driven by downwelling, as the TN flux from other sources differed by two to three orders of magnitude. In Santa Barbara, the riverine inputs were relatively insignificant compared with the other sources (Table 5, Fig. 5). In Ventura, effluent, riverine runoff, and atmospheric deposition contributions to TN were an equivalent order of magnitude and differed by three orders of magnitude from downwelling (Table 5, Fig. 5). The San Diego subregion had a large contribution of TN from effluent and riverine runoff; the upwelling is at the edge of the model boundary and is likely underestimated.

The absolute and standard error estimates were calculated to determine the amount of uncertainty in the nutrient source loads and fluxes (Table 4). The standard error determined for riverine runoff and effluent loads was less than 20% with one exception, the riverine runoff (wet weather) NH_4 loads (37.8%). Effluent loads from POTWs are monitored on a monthly basis and have been tracked over the last 30 yr with a high level of quality assurance (Lyon and Stein 2008). There were insufficient data to calculate the error for the atmospheric deposition estimates, but this appears to be a very small source at the subregional scale. The coupled ROMS and NPZD model has been validated at the 15-km resolution for the entire U.S. West Coast by comparing model results with either remote-sensing observations (from advanced very-high-resolution radiometer, sea-viewing wide field-of-view sensor) or in situ measurements from the California Cooperative Oceanic Fisheries Investigations Program (Gruber et al. 2006). Although we have a high level of confidence in our results at an annual and bight-wide scale, the 1-km ROMS model and NPZD used for the subregional scales has not yet been fully validated; therefore it is not possible at this time to calculate the error associated with the upwelling estimates from this study.

The two most urbanized subregions, Santa Monica Bay and San Pedro, had the largest percent change in TN flux due to anthropogenic sources (110% and 52%, respectively), whereas the less urbanized regions of Santa Barbara, Ventura, and North San Diego had much smaller changes in TN flux (1%, 1%, and 5%, respectively) due to anthropogenic inputs (Table 7). These findings contradict the current perception that anthropogenic nutrient inputs are negligible in upwelling-dominated regions. Other studies in Central California have focused on terrestrial runoff as the main source of anthropogenic nutrients (Kudela and Cochlan 2000; Kudela et al. 2008), but the results from this study show that wastewater inputs comprise a much higher contribution to the overall TN fluxes in the SCB, whereas the riverine contributions were relatively insignificant.

The importance of nutrient forms and ratios—Nitrogen is considered to be the primary limiting macronutrient for the growth of algae in many coastal ecosystems (Dugdale 1967; Ryther and Dunstan 1971), including California (Eppley et al. 1979). Previous studies have shown that the form of N, not just the quantity, is important for algal community composition, giving rise to algal blooms and HABs in particular (Howard et al. 2007; Cochlan et al. 2008; Kudela et al. 2008). The sources of N to the SCB are comprised of different forms of N, mainly NO_3, NH_4, and ON, which includes urea. When we examined the forms of N that comprised each of the sources examined in this study on a bight-wide scale, upwelling was mostly comprised of NO_3 (98.7% of TN), effluent was mostly comprised of NH_4 (92% of TN), and riverine runoff was comprised of a mixture of inorganic and organic N forms (34% and 60%, respectively; Table 3). ON was mostly derived from riverine runoff (60% on a bight-wide scale). NO_3 comprised only 7% of the TN load for effluent on a bight-wide scale (Table 3). However, examination of the forms of N from each source on a subregional scale provided surprising results (Table 6). In the heavily urbanized areas of Santa Monica Bay and San Pedro, effluent actually contributed a larger or equivalent NO_3 flux than riverine runoff or atmospheric deposition (Table 6, Fig. 5). These findings contradict the perception that the contribution of effluent NO_3 is insignificant, and show that effluent does provide an equivalent or larger contribution of NO_3 compared with riverine and atmospheric deposition sources. Upwelling was one to two orders of magnitude larger than all of the sources and thus clearly provided the largest contribution of NO_3 to the SCB (Table 6).

Urea, an organic form of N used as an indicator of coastal runoff in agricultural regions (Kudela and Cochlan 2000), has been found to sustain HABs in Central and Southern California (Kudela and Cochlan 2000; Kudela et al. 2008), and California HAB species have been shown to utilize urea for growth (McCarthy 1972; Howard et al.

2007). Despite these studies, urea concentrations in California's coastal waters and the importance of urea as an N source for algal growth is often overlooked and understudied. The main source of urea to the SCB was determined to be riverine runoff. Although it was a measurable source of N in the SCB, it was a minor component of the TN load (Tables 3, 6; Figs. 4, 5).

The nutrient fluxes estimated for the four major sources in this study were calculated at annual timescales. However, it is important to recognize that nutrient delivery to the coastal ocean on short, daily to weekly timescales is more ecologically relevant for primary productivity and HAB development. The timing of these nutrient inputs should be considered as some sources are chronic (daily wastewater effluent discharge into oceans and into rivers), whereas other sources are seasonal or episodic (riverine runoff and upwelling). Therefore, seasonal differences exist in both the TN flux as well as the proportion of N forms from each source. Riverine runoff is generally prevalent in the winter; upwelling occurs primarily in the spring and early summer; and effluent is chronic. Therefore, although upwelling clearly provided the largest source of NO_3 (Table 6, Fig. 5), effluent probably provided most of the NO_3 during nonupwelling and low riverine flow time periods. Other studies in SC have shown that stormwater runoff has at times been the dominant source of N inputs during nonupwelling periods and that those processes provided different proportions of N forms than upwelling (Warrick et al. 2005; McPhee-Shaw et al. 2007). In Monterey Bay, a more extensive study of this dynamic has shown similar results where riverine inputs of NO_3 exceeded upwelling inputs across short, daily to weekly, timescales (but not monthly or annual scales), as often as 28% of the year (Quay 2011).

Another aspect to consider from this study is the importance of N : P ratios. Although the conventional Redfield ratio of N : P is 16 : 1, the effluent sources in this study have disproportionate N : P ratios that widely varied by POTW. The two large POTWs located in the San Pedro subregion have the highest N : P ratios of 60 : 1 (JWPCP) and 21 : 1 (Treatment Plant No. 2). Given the large contribution of effluent to the TN flux in this subregion (Table 6, Fig. 5), these ratios suggest that effluent provides a disproportionate amount of N relative to P compared with natural sources.

Implications for primary production and algal blooms—Nitrogen is the primary limiting macronutrient in the coastal waters in the SCB (Eppley et al. 1979); consequently, any N inputs to the coastal oceans will likely increase biological productivity. The results from the subregional spatial scale of this study are more ecologically relevant to the development of algal blooms, and show that anthropogenic nutrients can provide a significant source of N for algal blooms, including HABs (Table 6, Fig. 5). Recent studies have identified chronic algal bloom hot spots that coincide with areas in the SCB that have major anthropogenic sources of nutrients (Nezlin et al. 2012), suggesting that at local spatial scales, anthropogenic nutrients may provide favorable growth conditions for algal bloom development. On a more refined spatial scale, terrestrial freshwater discharge and wastewater effluent discharges via ocean outfalls have been shown to increase phytoplankton biomass and affect patterns of phytoplankton productivity and community composition (Corcoran et al. 2010; Reifel et al. 2013). A 2006 study in Santa Monica Bay documented an effluent plume and urban riverine runoff that stimulated an algal bloom for which several HAB species dominated the community composition (Reifel et al. 2013). Other SCB studies in Santa Monica Bay and San Diego have been unable to attribute chlorophyll variability in the nearshore environment with upwelling and have concluded that nearshore productivity and chlorophyll are not always driven by classical coastal upwelling (Kim et al. 2009; Corcoran et al. 2010; Nezlin et al. 2012). The Scripps Pier time series in La Jolla, California (San Diego subregion) documented increased annual mean chlorophyll over the last 18 yr, but there was no obvious simultaneous increase in upwelling (Kim et al. 2009). Although anthropogenic nutrient sources (especially wastewater effluent) have traditionally been ignored as a significant source of N when evaluating algal biomass and community composition in the nearshore environment, the results from this study show that effluent contributes a significant portion of the TN flux, and therefore could explain nearshore chlorophyll variability that is not correlated to natural oceanographic conditions.

In summary, the results from this study contradict the currently held perception that anthropogenic nutrient inputs are negligible in upwelling-dominated regions and are consistent with a growing number of studies that suggest a linkage between anthropogenic N sources and HABs in California nearshore waters (Kudela and Cochlan 2000; Beman et al. 2005; Kudela et al. 2008). Although this study was designed to be a first-order estimation of nutrient sources, the results suggest that anthropogenic nutrients are not negligible compared with natural nutrients and can have ecological effects at local spatial scales. In the urbanized SCB, treated effluent has altered the quantity and composition of the N pool, which may have ecological consequences reflected in changes in algal community composition and has likely increased nearshore primary productivity and the duration of algal blooms. Although there are global examples of increased primary productivity with increased N inputs, quantification of such increases due to anthropogenic sources and determination of the spatial scale for which anthropogenic sources remain a significant component of overall TN in the SCB will be important to evaluate further in future research. The combination of physical and biogeochemical models will provide an important next step toward addressing these aspects of the effects of anthropogenic nutrients in the coastal waters of the SCB. Given that the forms of N can be biologically transformed, an important aspect of future studies should be to determine rates of nitrification and the timescales by which effluent NH_4 is transformed into NO_3, as these processes will alter the forms of N present. Future studies should also include a multiyear source analysis to determine the interannual variability for each source.

Acknowledgments

We express our gratitude to Becky Schaffner for assistance with map preparation. We thank the two anonymous reviewers as our manuscript was greatly improved from their suggestions and feedback.

This research was supported by funding provided by the California Ocean Protection Council (Grant Agreement 08-095), the State Water Resources Control Board (Agreement 08-060-250), and NOAA Monitoring and Event Response for HABs (NA05NO54781228).

References

Ackerman, D., and K. Schiff. 2003. Modeling stormwater mass emissions to the Southern California Bight. J. Am. Soc. Civ. Eng. **129:** 308–323, doi:10.1061/(ASCE)0733-9372(2003)129:4(308)

Anderson, D. M., P. M. Glibert, and J. M. Burkholder. 2002. Harmful algal blooms and eutrophication: Nutrient sources, composition, and consequences. Estuaries **25:** 704–726, doi:10.1007/BF02804901

Beman, M., K. Arrigo, and P. Matson. 2005. Agricultural runoff fuels large phytoplankton blooms in vulnerable areas of the ocean. Nature **434:** 211–214, doi:10.1038/nature03370

Burkov, V. A., and Y. V. Pavlova. 1980. Description of the eddy field of the California Current. [Translated from Russian.] Oceanology **20:** 272–278.

Caron, D. A., and others. 2010. Harmful algae and their potential impacts on desalination operations off southern California. J. Water Res. **44:** 385–416, doi:10.1016/j.watres.2009.06.051

Chisholm, J. R. M., F. E. Fernex, D. Mathieu, and J. M. Jaubert. 1997. Wastewater discharge, seagrass decline and algal proliferation on the Cote d' Azur. Mar. Poll. Bull. **34:** 78–84, doi:10.1016/S0025-326X(96)00072-0

Cochlan, W. P., J. Herndon, and R. M. Kudela. 2008. Inorganic and organic nitrogen uptake by the toxigenic diatom *Pseudo-nitzschia australis* (Bacillariophyceae). Harmful Algae **8:** 111–118, doi:10.1016/j.hal.2008.08.008

Conil, S., and A. Hall. 2006. Local regimes of atmospheric variability: A case study of Southern California. J. Clim. **19:** 4308–4325, doi:10.1175/JCLI3837.1

Corcoran, A. A., K. M. Reifel, B. H. Jones, and R. F. Shipe. 2010. Spatiotemporal development of physical, chemical, and biological characteristics of stormwater plumes in Santa Monica Bay, California (USA). J. Sea Res. **63:** 129–142, doi:10.1016/j.seares.2009.11.006

Dailey, M. D., J. W. Anderson, D. J. Reish, and D. S. Gorsline. 1993. The Southern California Bight: Background and setting, p. 1–18. *In* M. D. Dailey, D. J. Reish, and J. W. Anderson [eds.], Ecology of the Southern California Bight. Univ. of California Press.

Dong, C., E. Y. Idica, and J. C. McWilliams. 2009. Circulation and multiple-scale variability in the Southern California Bight. Prog. Oceanogr. **82:** 168–190, doi:10.1016/j.pocean.2009.07.005

Dorman, C. E., and C. D. Winant. 1995. Buoy observations of the atmosphere along the west coast of the United States. J. Geophys. Res. Oceans **100:** 16029–16044, doi:10.1029/95JC00964

Dugdale, R. C. 1967. Nutrient limitation in the sea: Dynamics, identification and significance. Limnol. Oceanogr. **12:** 685–695, doi:10.4319/lo.1967.12.4.0685

Egbert, G. D., A. F. Bennett, and M. G. G. Fore. 1994. Topex/Poseidon tides estimated using a global inverse model. J. Geophys. Res. **99:** 24821–24852, doi:10.1029/94JC01894

Eppley, R., E. Renger, and W. Harrison. 1979. Nitrate and phytoplankton production in California coastal waters. Limnol. Oceanogr. **24:** 483–494, doi:10.4319/lo.1979.24.3.0483

Fasham, M. J. R., H. W. Ducklow, and S. M. McKelvie. 1990. A nitrogen-based model of plankton dynamics in the oceanic mixed layer. J. Mar. Res. **48:** 591–639, doi:10.1357/002224090784984678

Garcia, H. E., R. A. Locarnini, T. P. Boyer, and J. I. Antonov. 2006. Nutrients (phosphate, nitrate, and silicate), p. 396. *In* S. Levitus [ed.], World Ocean Atlas 2005, V. 4. NOAA Atlas NESDIS 64, U.S. Government Printing Office.

Glibert, P. M., J. Harrison, C. Heil, and S. Seitzinger. 2006. Escalating worldwide use of urea—a global change contributing to coastal eutrophication. Biogeochemistry **77:** 441–463, doi:10.1007/s10533-005-3070-5

———, S. Seitzinger, C. A. Heil, J. M. Burkholder, M. W. Parrow, L. A. Codispoti, and V. Kelly. 2005. The role of eutrophication in the global proliferation of harmful algal blooms. Oceanography **18:** 198–209, doi:10.5670/oceanog.2005.54

Goeyens, L., N. Kindermans, M. Abu Yusuf, and M. Elskens. 1998. A room temperature procedure for the manual determination of urea in seawater. Est. Coast. Shelf Sci. **47:** 415–418, doi:10.1006/ecss.1998.0357

Gruber, N., and others. 2006. Eddy-resolving simulation of plankton ecosystem dynamics in the California Current System. Deep Sea Res. I **53:** 1483–1516, doi:10.1016/j.dsr.2006.06.005

Hallegraeff, G. M. 2004. Harmful algal blooms: A global overview, p. 25–49. *In* G. M. Hallegraeff, D. M. Anderson, and A. D. Cembella [eds.], Manual on harmful marine microalgae. UNESCO Publishing.

Hamilton, P., M. A. Noble, J. Largierc, L. K. Rosenfeld, and G. Robertson. 2006. Cross-shelf subtidal variability in San Pedro Bay during summer. Cont. Shelf Res. **26:** 681–702, doi:10.1016/j.csr.2006.01.009

Heisler, J., and others. 2008. Eutrophication and harmful algal blooms: A scientific consensus. Harmful Algae **8:** 3–13, doi:10.1016/j.hal.2008.08.006

Hickey, B. M. 1979. The California Current system: Hypotheses and facts. Prog. Oceanogr. **8:** 191–279, doi:10.1016/0079-6611(79)90002-8

———. 1992. Circulation over the Santa Monica–San Pedro basin and shelf. Prog. Oceanogr. **30:** 37–115, doi:10.1016/0079-6611(92)90009-O

Howard, M. D. A., W. P. Cochlan, R. M. Kudela, and N. Ladizinsky. 2007. Nitrogenous preference of toxic *Pseudo-nitzschia australis* (Bacillariophyceae) from field and laboratory experiments. Harmful Algae **6:** 206–217, doi:10.1016/j.hal.2006.06.003

———, and others. 2012. Southern California Bight 2008 Regional Monitoring Program: Volume IX. Water Quality. Technical Report 710. Southern California Coastal Water Research Project. Costa Mesa, CA.

Howarth, R. W. 2008. Coastal nitrogen pollution: A review of sources and trends globally and regionally. Harmful Algae **8:** 14–20, doi:10.1007/BF02804898

Jaubert, J. M., J. R. M. Chisholm, A. Minghelli-Roman, M. Marchioretti, J. H. Morrow, and H. T. Ripley. 2003. Re-evaluation of the extent of *Caulerpa taxifolia* development in the northern Mediterranean using airborne spectrographic sensing. Mar. Ecol. Progr. Ser. **263:** 75–82, doi:10.3354/meps263075

Kim, H. J., A. J. Miller, J. McGowan, and M. L. Carter. 2009. Coastal phytoplankton blooms in the Southern California Bight. Prog. Oceanogr. **82:** 137–147, doi:10.1016/j.pocean.2009.05.002

Kondo, J. 1975. Air–sea bulk transfer coefficients in diabatic condition. Bound.-Layer Meteor. **9:** 91–112.

Kudela, R. M., and W. P. Cochlan. 2000. The kinetics of nitrogen and carbon uptake and the influence of irradiance for a natural population of *Lingulodinium polyedrum* (Pyrrophyta) off Southern California. Aquat. Microbial Ecol. **21:** 31–47, doi:10.3354/ame021031

———, J. Q. Lane, and W. P. Cochlan. 2008. The potential role of anthropogenically derived nitrogen in the growth of harmful algae in California, USA. Harmful Algae **8:** 103–110, doi:10.1016/j.hal.2008.08.019

Lange, C. B., F. M. H. Reid, and M. Vernet. 1994. Temporal distribution of the potentially toxic diatom *Pseudo-nitzschia australis* at a coastal site in Southern California. Mar. Ecol. Prog. Ser. **104:** 309–312, doi:10.3354/meps104309

Large, W. G., and S. Pond. 1981. Open ocean momentum flux measurements in moderate to strong winds. J. Phys. Oceanogr. **11:** 324–336, doi:10.1175/1520-0485(1981)011<0324:OOMFMI>2.0.CO;2

Lapointe, B., P. J. Barile, M. M. Littler, and D. S. Littler. 2005. Macroalgal blooms on southeast Florida coral reefs II. Cross-shelf discrimination of nitrogen sources indicates widespread assimilation of sewage nitrogen. Harmful Algae **4:** 1106–1122, doi:10.1016/j.hal.2005.06.002

Lapointe, B. E., P. J. Barile, and W. R. Matzie. 2004. Anthropogenic nutrient enrichment of seagrass and coral reef communities in the lower Florida keys: Discrimination of local versus regional nitrogen sources. J. Exp. Mar. Biol. Ecol. **308:** 23–58, doi:10.1016/j.jembe.2004.01.019

Lewitus, A. J., and others. 2012. Harmful algal blooms along the North American west coast region: History, trends, causes and impacts. Harmful Algae **19:** 133–159, doi:10.1016/j.hal.2012.06.009

Lyon, G. S., and E. D. Stein. 2008. Effluent discharges to the Southern California Bight from small municipal wastewater treatment facilities in 2005, p. 1–14. *In* S. B. Weisberg and K. Miller [eds.], Southern California coastal water research project 2008 annual report. Southern California Coastal Water Research Project.

Marchesiello, P., J. C. McWilliams, and A. F. Shchepetkin. 2003. Equilibrium structure and dynamics of the California Current system. J. Phys. Oceanogr. **33:** 753–783, doi:10.1175/1520-0485(2003)33<753:ESADOT>2.0.CO;2

McCarthy, J. J. 1972. The uptake of urea by natural populations of marine phytoplankton. Limnol. Oceanogr. **17:** 738–748, doi:10.4319/lo.1972.17.5.0738

McPhee-Shaw, E. E., D. A. Siegel, L. Washburn, M. A. Brzezinski, J. L. Jones, A. Leydecker, and J. Melack. 2007. Mechanisms for nutrient delivery to the inner shelf: Observations from the Santa Barbara Channel. Limnol. Oceanogr. **52:** 1748–1766, doi:10.4319/lo.2007.52.5.1748

Moumen, N., S.-M. Yi, H. A. Raymond, Y. J. Han, and T. M. Holsen. 2004. Quantifying the dry deposition of ammonia in ammonia-rich and ammonia-poor environments using a surrogate surface approach. Atmos. Environ. **38:** 2677–2686, doi:10.1016/j.atmosenv.2004.02.010

Nezlin, N. P., M. A. Sutula, R. P. Stumpf, and A. Sengupta. 2012. Phytoplankton blooms detected by SeaWiFS along the central and southern California Coast. J. Geophys. Res. **117:** C07004, doi:10.1029/2011JC007773

O'Loughlin, G., W. Huber, and B. Chocat. 1996. Rainfall-runoff processes and modeling. J. Hydr. Res. **34:** 733–751, doi:10.1080/00221689609498447

Paerl, H. W., and M. F. Piehler. 2008. Nitrogen and marine eutrophication, p. 529–567. *In* D. Capone, D. Bronk, M. Mulholland, and E. Carpenter [eds.], Nitrogen in the marine environment. Elsevier.

Quay, J. 2011. New tools and insight for the recognition of *Pseudo-nitzschia* blooms and toxin incidence. Ph.D. thesis. Univ. of California, Santa Cruz.

Raymond, H. A., S.-M. Yi, N. Moumen, Y. J. Han, and T. M. Holsen. 2004. Quantifying the dry deposition of reactive nitrogen and sulfur-containing species in remote areas using a surrogate surface analysis approach. Atmos. Environ. **38:** 2687–2697, doi:10.1016/j.atmosenv.2004.02.011

Reifel, K. M., A. A. Corcoran, C. Cash, R. Shipe, and B. H. Jones. 2013. Effects of a surfacing effluent plume on a coastal phytoplankton community. Cont. Shelf Res. **60:** 38–50, doi:10.1016/j.csr.2013.04.012

Ryther, J., and W. Dunstan. 1971. Nitrogen, phosphorus and eutrophication in the coastal marine environment. Science **171:** 1008–1112, doi:10.1126/science.171.3975.1008

Sandwell, D. T. 1987. Biharmonic spline interpolation of GEOS-3 and SEASAT altimeter data. Geophys. Res. Lett. **14:** 139–142, doi:10.1029/GL014i002p00139

Schnetzer, A., and others. 2007. Blooms of *Pseudo-nitzschia* and domoic acid in the San Pedro Channel and Los Angeles harbor areas of the Southern California Bight, 2003–2004. Harmful Algae **6:** 372–387, doi:10.1016/j.hal.2006.11.004

———, and ———. 2013. Coastal upwelling linked to toxic *Pseudo-nitzschia australis* blooms in Los Angeles coastal waters, 2005–2007. J. Plankton Res. **35:** 1080–1092, doi:10.1093/plankt/fbt051

Seubert, E. L., and others. 2013. Seasonal and annual dynamics of harmful algae and algal toxins revealed through weekly monitoring at two coastal ocean sites off southern California, USA. Environ. Sci. Pollut. Res. **20:** 6878–6895, doi:10.1007/s11356-012-1420-0

Shchepetkin, A. F., and J. C. McWilliams. 2005. The regional oceanic modeling system (ROMS): A split-explicit, free-surface, topography-following-coordinate oceanic model. Ocean Mod. **9:** 347–404, doi:10.1016/j.ocemod.2004.08.002

Song, Y., and D. B. Haidvogel. 1994. A semi-implicit ocean circulation model using a generalized topography-following coordinate system. J. Comp. Phys. **115:** 228–244, doi:10.1006/jcph.1994.1189

Stein, E. D., L. L. Tiefenthaler, and K. C. Schiff. 2007. Sources, patterns and mechanisms of storm water pollutant loading from watersheds and land uses of the greater Los Angeles area, California, USA. Technical Report 510. Costa Mesa: Southern California Coastal Water Research Project.

Sverdrup, H. U., and R. H. Fleming. 1941. The waters off the coast of southern California, March to July 1937. Bulletin of the Scripps Institution of Oceanography **4:** 261–378.

Thompson, P., and A. Waite. 2003. Phytoplankton responses to wastewater discharges at two sites in Western Australia. Mar. Freshw. Res. **54:** 721–735, doi:10.1071/MF02096

Trainer, V., and others. 2000. Domoic acid production near California coastal upwelling zones, June 1998. Limnol. Oceanogr. **45:** 1818–1833, doi:10.4319/lo.2000.45.8.1818

Warrick, J., L. Washburn, M. Brzezinski, and D. Siegel. 2005. Nutrient contributions to the Santa Barbara Channel, California, from the ephemeral Santa Clara River. Est. Coast. Shelf Sci. **62:** 559–574, doi:10.1016/j.ecss.2004.09.033

Associate editor: Mary I. Scranton

Received: 02 March 2013
Accepted: 03 September 2013
Amended: 02 November 2013